Research Square

Preprints are preliminary reports that have not undergone peer review.
They should not be considered conclusive, used to inform clinical practice,
or referenced by the media as validated information.

Disulfiram attenuates paraquat-induced hepatic injury and fibrotic remodeling by reducing oxidative stress and modulating NLRP3 and PGC-1α expression in rats

Hanieh Moghimi Kandelousi
Babol University of Medical Sciences
Mahtab Esmaeili
Babol University of Medical Sciences
Hossein Najafzadehvarzi
Babol University of Medical Sciences
Abdolreza Daraei
Babol University of Medical Sciences
Zohre Esmaeili
Babol University of Medical Sciences
Zahra Babazadeh
zbabazadeh1400@gmail.com

Babol University of Medical Sciences

Research Article

Keywords: Disulfiram, Paraquat, Hepatic Fibrosis, Oxidative Stress, NLRP3 Inflammasome, PGC-1α, Liver Injury

Posted Date: November 13th, 2026

DOI: https://doi.org/10.21203/rs.3.rs-11568410/v1

License: This work is licensed under a Creative Commons Attribution 4.0 International License.
Read Full License

Additional Declarations: No competing interests reported.

Disulfiram attenuates paraquat-induced hepatic injury and fibrotic remodeling by reducing oxidative stress and modulating NLRP3 and PGC-1α expression in rats

Running title: DSF and PQ-induced liver injury: NLRP3/PGC-1α axis

Hanieh Moghimi Kandelousi[1,2], Mahtab Esmaeili [1,2], Hossein Najafzadehvarzi [2,3,] Abdolreza Daraei [2,4], Zohre Esmaeili [2,5], Zahra Babazadeh [2,5*]

1-Student Research Committee, Babol University of Medical Sciences, Babol, Iran;

2-Cellular and Molecular Biology Research Center, Health Research Institute, Babol University of Medical Sciences, Babol, Iran

3- Department of Pharmacology, Faculty of Medicine, Babol University of Medical Sciences, Babol, Iran

4-Department of Medical Genetics, School of Medicine, Babol University of Medical Sciences, Babol, Iran

5-Department of Anatomical Sciences, School of Medicine, Babol University of Medical Sciences, Babol, Iran

Corresponding Author: Zahra Babazadeh

zbabazadeh1400@gmail.com

z.babazadeh@mubabol.ac.ir

Zahra Babazadeh ORCID: 0000-0002-0399-6937

Najafzadeh ORCID: 0000-0002-3686-7170

Abdolreza Daraei ORCID: 0000-0002-2106-835X

Zohre Esmaeili ORCID: 0009-0000-9919-4834

Abstract

Purpose: Paraquat (PQ) is a highly toxic herbicide that induces hepatic injury through oxidative stress, inflammasome activation, and progressive fibrosis, contributing to chronic liver disease. Drug repurposing offers a promising strategy for accelerating therapeutic development. This study evaluated the hepatoprotective and antifibrotic potential of disulfiram (DSF), a clinically approved drug with emerging antioxidant and anti-

inflammatory properties, against PQ-induced hepatic injury, including its association with NLRP3 inflammasome activation and PGC-1α expression.

Methods: Thirty-five male Wistar rats were randomly assigned to seven groups: Control, Vehicle, DSF20, PQ (1.5 mg/kg), and PQ co-treated with DSF (5, 10, or 20 mg/kg). PQ and DSF were administered via intraperitoneal injection for 4 weeks (5 consecutive days per week, with 2-day intervals). Hepatic injury was evaluated using histopathology (H&E and Masson's trichrome staining), serum biomarkers (ALT, AST, and ALP), oxidative stress parameters (malondialdehyde [MDA], catalase [CAT], and glutathione peroxidase [GPx]), NLRP3 and PGC-1α gene expression determined by qRT-PCR, and quantitative fibrosis assessment (fibrosis score and fibrotic area percentage).

Results: PQ exposure caused marked hepatic histopathological injury, increased oxidative stress, elevated liver enzymes, increased NLRP3 expression, decreased PGC-1α expression, and elevated fibrosis. DSF co-treatment, particularly at 20 mg/kg, significantly ameliorated these changes by reducing tissue injury, lowering lipid peroxidation, restoring antioxidant enzyme activity, suppressing NLRP3 expression, restoring PGC-1α expression, and decreasing fibrosis score and fibrotic area. Notably, NLRP3 suppression was effective at both 10 and 20 mg/kg, whereas a significant reduction in fibrosis required 20 mg/kg.

Conclusion: Disulfiram, particularly at 20 mg/kg, significantly attenuated PQ-induced hepatic injury and fibrotic remodeling, accompanied by reduced oxidative stress, suppression of NLRP3 expression, and restoration of PGC-1α expression.

Keywords: Disulfiram; Paraquat; Hepatic Fibrosis; Oxidative Stress; NLRP3 Inflammasome; PGC-1α; Liver Injury

Introduction

The liver is a central organ responsible for metabolic homeostasis, xenobiotic metabolism, detoxification, and immune regulation, making it particularly vulnerable to environmental and chemical toxicants. Persistent hepatocellular injury can initiate oxidative and inflammatory responses that, when sustained, promote tissue remodeling and excessive extracellular matrix deposition, ultimately contributing to hepatic fibrosis and progression

of chronic liver disease. Oxidative stress and inflammation are therefore closely interconnected processes in the initiation and progression of hepatic injury and fibrotic remodeling [1, 2].

Paraquat (PQ) is a widely used bipyridyl herbicide and potent environmental toxicant capable of causing injury to multiple organs, including the liver. Experimental evidence indicates that PQ exposure induces biochemical and histopathological abnormalities accompanied by substantial oxidative stress. A major mechanism underlying PQ toxicity is redox cycling, which promotes excessive generation of reactive oxygen species (ROS), lipid peroxidation, and disruption of cellular antioxidant defenses. In a rat model of PQ-induced acute liver injury, PQ exposure increased hepatic malondialdehyde (MDA) levels and produced biochemical and histopathological evidence of liver damage. Importantly, PQ exposure was also associated with activation of the NOD-LRR-pyrin domain-containing protein 3 (NLRP3) inflammasome, supporting a mechanistic link between oxidative stress and inflammatory signaling in PQ-induced hepatic injury [3].

The NLRP3 inflammasome is a key component of innate immune signaling that responds to cellular stress and damage-associated signals, including excessive ROS production and lysosomal dysfunction. Upon activation, NLRP3 promotes caspase-1 activation and maturation of pro-inflammatory cytokines, particularly interleukin (IL)-1β and IL-18, thereby amplifying inflammatory responses and, under certain conditions, promoting pyroptotic cell death. Increasing evidence also implicates NLRP3-associated signaling in hepatic fibrotic remodeling. In experimental liver fibrosis, inhibition of NLRP3 activation has been associated with attenuation of inflammatory responses and reduction of fibrotic changes, highlighting the potential relevance of this pathway to the progression of hepatic injury and fibrosis [4].

Mitochondrial homeostasis represents another critical determinant of hepatic responses to oxidative and metabolic stress. Peroxisome proliferator-activated receptor gamma coactivator 1-alpha (PGC-1α) is a transcriptional coactivator that regulates mitochondrial biogenesis, oxidative metabolism, and cellular energy homeostasis. Impaired PGC-1α signaling has been associated with mitochondrial dysfunction, oxidative stress, and hepatic fibrotic remodeling, whereas preservation of PGC-1α activity may contribute to maintaining mitochondrial function during chronic liver injury [5, 6]. Thus, assessment of PGC-1α alongside oxidative and inflammatory markers may provide complementary insight into the cellular responses associated with toxicant-induced hepatic damage.

Disulfiram (DSF) is an established pharmacological treatment for alcohol use disorder that has attracted increasing interest because of biological activities extending beyond its classical therapeutic indication. Experimental studies have demonstrated anti-inflammatory and anti-pyroptotic effects of DSF and its metabolites, including modulation of intracellular ROS production and NLRP3 inflammasome activation [7, 8]. In particular, DSF has been shown to suppress NLRP3 inflammasome activation and pyroptotic cell death, with inhibition of lysosomal cathepsin B release and reduction of ROS production proposed as contributing mechanisms [9]. These findings provide a mechanistic rationale for investigating DSF as a potential modulator of oxidative stress-associated inflammatory injury.

Importantly, however, the hepatic effects of DSF are not uniformly protective. Disulfiram is a well-established cause of clinically apparent drug-induced liver injury, with reported manifestations ranging from asymptomatic aminotransferase elevations to acute hepatitis, jaundice, and, in severe cases, acute liver failure and death [10]. Histopathological findings in reported cases include portal inflammation, eosinophilic infiltration, and hepatocellular necrosis, supporting a clinically relevant hepatotoxic potential of DSF [11]. The mechanism of DSF hepatotoxicity is considered predominantly idiosyncratic and may involve immune-mediated responses and toxic metabolites. These observations are particularly important when evaluating DSF in experimental models of liver injury, because a protective effect cannot be assumed solely from its anti-inflammatory properties [12].

Conversely, experimental studies have demonstrated hepatoprotective and antifibrotic effects of DSF under specific pathological conditions. DSF encapsulated in polymer nanoparticles ameliorated thioacetamide-induced liver injury and reduced inflammatory responses [13]. Similarly, low-dose DSF (4 mg/kg) attenuated CCl_4- and bile duct ligation-induced liver fibrosis in rats, accompanied by suppression of hepatic stellate cell activation and viability [14]. DSF has also been reported to attenuate acetaminophen-induced acute liver injury by modulating the gut microbiota and PI3K/Akt signaling [15]. More recently, a rat study using CCl_4-induced liver fibrosis found that DSF at 25 mg/kg reduced ALT, AST, and MDA levels and improved hepatocyte morphology. In contrast, neither 25 nor 50 mg/kg significantly reduced collagen deposition [16]. Together, these findings indicate that the hepatic effects of DSF may vary according to the underlying toxicant, dose, duration, and biological context, with both hepatotoxic and hepatoprotective outcomes reported.

This apparent context dependence highlights an important unresolved question regarding the effects of DSF in toxicant-induced hepatic injury. Although DSF has been reported to exert anti-inflammatory and hepatoprotective effects in some experimental models, its effects may vary depending on the underlying pathological context. Whether DSF can protect against PQ-induced hepatic injury and fibrotic remodeling, and whether such effects are associated with modulation of oxidative stress, NLRP3-associated inflammation, and PGC-1α-related mitochondrial homeostasis, remains unclear. Therefore, the present study aimed to investigate the potential hepatoprotective effects of DSF in PQ-induced liver injury and to clarify the molecular pathways that may underlie its effects.

2- Methods and Materials

2.1. Animal Care and Experimental Design

2.1.1. Animal Care and Housing

All animal procedures in the present study were approved by the Institutional Animal Care and Use Committee of Babol University of Medical Sciences (Approval code: IR.MUBABOL.AEC.1403.021) and were conducted in accordance with institutional guidelines for the care and use of laboratory animals. A total of 35 healthy male Wistar rats (8 ± 1 weeks old, 200 ± 20 g) were obtained from the Laboratory Animal Center. The animals were housed under controlled environmental conditions (22 ± 3 °C, 55 ± 10% humidity, and a 12-h light/dark cycle), with free access to standard rodent chow (Pars Animal Feed Co., Tehran, Iran) and tap water. All efforts were made to minimize animal suffering and reduce the number of animals used.

2.1.2. Experimental Design and Treatment Protocol

The 35 rats were randomly allocated into seven groups (n = 5 per group): (1) Control, receiving no treatment; (2) Vehicle, receiving olive oil (200 µL/day, i.p.); (3) DSF20, receiving disulfiram alone (20 mg/kg/day, i.p.); (4) PQ, receiving paraquat (1.5 mg/kg/day, p.o.); (5) PQ+DSF5, receiving paraquat (1.5 mg/kg/day, p.o.) plus disulfiram (5 mg/kg/day, i.p.); (6) PQ+DSF10, receiving paraquat (1.5 mg/kg/day, p.o.) plus disulfiram (10 mg/kg/day, i.p.); and (7) PQ+DSF20, receiving paraquat (1.5 mg/kg/day, p.o.) plus disulfiram (20 mg/kg/day, i.p.). The paraquat dose of 1.5 mg/kg/day was selected based on previous experimental studies demonstrating that repeated exposure to this

dose induces hepatic injury in rats [17, 18]. All treatments were administered once daily, 5 consecutive days per week, with 2-day intervals, for a total experimental period of 4 weeks [19].

Following completion of the 4-week treatment period, rats were anesthetized with ketamine (80 mg/kg) and xylazine (10 mg/kg), and blood was collected by cardiac puncture. Euthanasia was completed by exsanguination and confirmed by bilateral thoracotomy. Blood samples were allowed to clot for 30 min at room temperature and centrifuged at 3000 rpm for 15 min, and the separated serum was stored at −80 °C until biochemical analysis. The liver was then immediately excised, with representative portions fixed in 10% neutral-buffered formalin for histopathological and fibrotic assessments, while additional samples were snap-frozen in liquid nitrogen and stored at −80 °C for biochemical and molecular analyses.

2.2. Histopathological Assessments

2.2.1: Tissue Processing and Staining

Fixed liver tissues were processed through graded ethanol solutions (70%, 80%, 90%, 96%, and 100%), cleared in xylene, and embedded in paraffin wax. Serial sections (4 μm) were cut using a rotary microtome (Leica RM2245, Germany) and mounted on glass slides.

For histopathological assessment, sections were stained with:

2.2.2: Hematoxylin and Eosin (H&E): Following deparaffinization and rehydration, sections were stained with Mayer's hematoxylin and eosin Y (Asiapajouhesh, Iran) according to standard protocols [16].

2.2.3: Masson’s Trichrome: Collagen deposition was assessed using a commercial kit (Asiapajouhesh, Iran; Cat. No. 140011) as per the manufacturer’s instructions [16].

2.2.4: Liver Histology Evaluation

Histopathological factors, including lobular structure deformation, cytoplasmic vacuolation, presence of necrotic cells, vascular congestion, and inflammatory cells, were graded based on the severity of liver tissue damage (0, absent; 1, mild intensity; 2, moderate intensity; 3, high intensity) [16, 20, 21]. Liver fibrosis was graded according to the Ishak fibrosis scoring system (0-6 grades) [22].

2.2.5: Quantification of hepatic necrosis and fibrosis

Liver sections stained with hematoxylin and eosin (H&E) and Masson's trichrome were used for quantification. For assessment of necrotic nuclei, H&E-stained liver sections were imaged at 18× magnification and analyzed using Fiji (ImageJ, NIH, Bethesda, MD, USA). The hematoxylin channel was isolated through color deconvolution (H&E vector) to enhance nuclear staining specifically. The deconvolved hematoxylin channel was then subjected to fixed thresholding uniformly applied to all sections to segment areas of nuclear loss, which are characteristic of necrotic regions. The necrotic-positive area fraction (%Area) was calculated for five randomly selected hepatic fields per animal.

For hepatic fibrosis, Masson's trichrome–stained liver sections were used. Collagen was isolated through color deconvolution (Masson's Trichrome vector), and the collagen channel was subjected to fixed thresholding uniformly applied to all sections. The collagen-positive area fraction (%Area) was calculated for five randomly selected hepatic fields per animal.

2.3. Molecular Analyses

2.3.1. Gene Expression Analysis of NLRP3 and PGC-1α

Approximately 30 mg of frozen liver tissue was homogenized, and total RNA was extracted using lysis buffer (ParsTous, Mashhad, Iran) according to the manufacturer's instructions. RNA concentration and purity were assessed spectrophotometrically using a NanoDrop spectrophotometer (Thermo Fisher Scientific, USA), and RNA integrity was evaluated by agarose gel electrophoresis.

First-strand cDNA was synthesized from 1 µg of total RNA using a commercial reverse transcription kit (YTA, Iran) in a final reaction volume of 20 µL, according to the manufacturer's protocol. Quantitative real-time PCR (qRT-PCR) was performed in triplicate using SYBR Green Master Mix (Ampliqon, Denmark) in a final volume of 20 µL. Each reaction contained 2 µL of cDNA template and 0.5 µM of each primer. Amplification was performed using a Mic qPCR Cycler (Bio Molecular Systems, Australia). The cycling conditions consisted of an initial denaturation step at 95 °C for 15 min, followed by 40 cycles of denaturation at 95 °C for 30 s, primer-specific annealing at 64 °C for NLRP3, 61 °C for PGC-1α, and 58 °C for GAPDH for 30 s, and extension at 72 °C for 30 s.

A melting-curve analysis was performed at the end of amplification to confirm the specificity of the PCR products. GAPDH was used as the reference gene, and relative gene expression was calculated using the 2^−ΔΔCt method. The primer sequences used for NLRP3, PGC-1α, and GAPDH are presented in Table 1.

Table 1. Primer sequences used for quantitative real-time PCR

Gene	Forward (5′–3′)	Reverse (5′–3′)
NLRP-3	CAGGATCTCGCATTGGTTCT	AGCAGCACAGTGAAGTAAGG
PGC-1α	CAACACTCAGCTCAGCTACAA	GCTCCATGAATTCTCGGTCTT
GAPDH	GACAGCCGCATCTTCTTGTG	GGTAACCAGGCGTCCGATAC

2.4. Biochemical Analyses

2.4.1. Measurement of Liver Enzymes

Blood samples (from cardiac) were centrifuged at 3000 rpm to separate the serum, which was aliquoted and stored at −80 °C until analysis. Serum alanine aminotransferase (ALT), aspartate aminotransferase (AST), and alkaline phosphatase (ALP) levels were determined using commercial diagnostic kits (Pars Azmoon Co., Iran) according to the manufacturer's instructions. Enzyme activities were measured spectrophotometrically.

2.4.2. Oxidative Stress Markers

Liver tissue samples were homogenized at a 10% (w/v) concentration in ice-cold phosphate-buffered saline (PBS; pH 7.4) using a glass–Teflon homogenizer. The homogenates were centrifuged at 12,000 rpm for 15 min at 4 °C, and the resulting supernatants were collected for biochemical analyses.

Catalase (CAT) activity was determined using a commercial kit (Kiazist, Hamedan, Iran) based on the decomposition of hydrogen peroxide (H_2O_2), with absorbance measured at 240 nm. Malondialdehyde (MDA), as an indicator of lipid peroxidation, was measured using the thiobarbituric acid-reactive substances (TBARS) method with a commercial kit (Kiazist, Hamedan, Iran). Glutathione peroxidase (GPx) activity was measured using a

commercial kit (Navand Salamat, Urmia, Iran), based on the reduction of cumene hydroperoxide coupled with NADPH oxidation, according to the manufacturer's instructions.

2.5. Statistical Analysis

All statistical analyses were performed using GraphPad Prism version 10.4.1 (GraphPad Software, USA). Histopathological lesion scores were analyzed using the Kruskal–Wallis test, followed by Dunn's multiple-comparisons test for pairwise comparisons.

Continuous variables, including serum biochemical parameters, oxidative stress markers, and relative gene-expression levels, were analyzed using one-way analysis of variance (ANOVA), followed by Tukey's multiple-comparisons test. The percentages of fibrotic and necrotic areas were analyzed using nested one-way ANOVA to account for measurements obtained from multiple microscopic fields within individual animals. Data are presented as mean ± standard error of the mean (SEM). A two-sided P value <0.05 was considered statistically significant**.**

3-Result

3-1: Histopathological findings

Histopathological evaluation demonstrated marked hepatic injury in the PQ group compared with the control group. PQ exposure significantly increased the scores of all assessed histopathological parameters, including lobular destruction, hepatocyte vacuolation, hepatocyte hyalinization, necrotic hepatocytes, central vein congestion, portal congestion, sinusoidal congestion, total congestion, sinusoidal collapse, and macrophage accumulation in the sinusoids, as well as the percentage of necrotic nuclei area (all $P<0.0001$).

DSF treatment significantly attenuated several PQ-induced cellular alterations. **Lobular destruction** was significantly reduced in the PQ+DSF5, PQ+DSF10, and PQ+DSF20 groups compared with the PQ group ($P=0.0402$, $P=0.0074$, and $P<0.0001$, respectively). The score was lowest in the PQ+DSF20 group (0.7586 ± 0.1460), which also differed significantly from the PQ+DSF5 group ($P=0.0320$). **Hepatocyte vacuolation** was significantly reduced in the PQ+DSF10 and PQ+DSF20 groups compared with the PQ group (both $P<0.0001$); significant differences were also observed between PQ+DSF5 and both PQ+DSF10 and PQ+DSF20 (both

P<0.0001). Similarly, **hepatocyte hyalinization** was significantly lower in the PQ+DSF10 and PQ+DSF20 groups than in the PQ group (P=0.0018 and P<0.0001, respectively), with a significant difference between PQ+DSF5 and PQ+DSF20 (P=0.0472). **Necrotic hepatocyte scores** were also significantly reduced in the PQ+DSF10 and PQ+DSF20 groups compared with the PQ group (both P<0.0001), while significant differences were observed between PQ+DSF5 and PQ+DSF10 (P=0.0009) and between PQ+DSF5 and PQ+DSF20 (P<0.0001). The **percentage of necrotic nuclei area** was significantly lower in the PQ+DSF10 and PQ+DSF20 groups than in the PQ group (2.146 ± 0.2218% and 1.599 ± 0.1141% vs. 6.539 ± 0.2978%; both P<0.0001). Significant differences were also observed between PQ+DSF5 and PQ+DSF10 and between PQ+DSF5 and PQ+DSF20 (both P<0.0001) (Fig. 1, 2).

DSF treatment also attenuated PQ-induced **vascular and sinusoidal alterations**. **Central vein congestion** was significantly reduced by DSF5, DSF10, and DSF20 compared with PQ (P=0.0003, P<0.0001, and P<0.0001, respectively), as was **portal congestion** (P=0.0018, P=0.0042, and P<0.0001, respectively). **Sinusoidal congestion** was significantly reduced in all three DSF-treated groups compared with PQ (P=0.0397, P<0.0001, and P<0.0001, respectively), with significant differences between PQ+DSF5 and PQ+DSF20 (P<0.0001) and between PQ+DSF10 and PQ+DSF20 (P=0.0011). **Total congestion** was also significantly lower in all DSF-treated groups than in the PQ group (all P<0.0001), with significant differences between PQ+DSF5 and PQ+DSF10 (P=0.0001) and between PQ+DSF10 and PQ+DSF20 (P=0.0225). **Sinusoidal collapse** was significantly reduced in the PQ+DSF10 and PQ+DSF20 groups compared with PQ (P=0.0025 and P<0.0001, respectively); significant differences were also observed between PQ+DSF5 and PQ+DSF20 (P<0.0001) and between PQ+DSF10 and PQ+DSF20 (P=0.0211). Finally, **macrophage accumulation in the sinusoids** was significantly reduced only in the PQ+DSF20 group compared with the PQ group (P=0.0039). (Fig. 2, 3).

3-2: Hepatic fibrosis

PQ exposure significantly increased hepatic fibrosis compared with the control group, as demonstrated by both the fibrosis score and the percentage of fibrotic area. The **fibrosis score** increased from 0.06000 ± 0.03393 in the control group to 3.717 ± 0.1090 in the PQ group (P<0.0001). Similarly, the **percentage of fibrotic area** increased from 3.221 ± 0.2279% in the control group to 17.08 ± 0.7621% in the PQ group (P<0.0001).

Treatment with DSF20 significantly reduced both measures of hepatic fibrosis compared with the PQ group. The fibrosis score decreased to 0.6269 ± 0.1038 in the PQ+DSF20 group (P<0.0001), while the percentage of fibrotic area decreased to 10.41 ± 0.5816% (P<0.0001). Significant differences were also observed between the PQ+DSF5 and PQ+DSF20 groups and between the PQ+DSF10 and PQ+DSF20 groups for both the fibrosis score and the percentage of fibrotic area (all P<0.0001). (Fig. 4, 5).

3-3: Gene Expressions

3.3.1: NLRP3 gene expression

In contrast, PQ exposure significantly increased NLRP3 gene expression compared with the Control group (5.836 ± 0.5855 vs. 1.050 ± 0.1696, P<0.0001; Fig. X). NLRP3 expression was significantly lower in the PQ+DSF10 and PQ+DSF20 groups than in the PQ group (2.297 ± 0.2803, P=0.0004; and 1.584 ± 0.3673, P<0.0001, respectively). Among the DSF-treated groups, NLRP3 expression was significantly lower in the PQ+DSF10 and PQ+DSF20 groups than in the PQ+DSF5 group (P=0.0103 and P=0.0007, respectively). (Fig. 6 a).

3.3.2: PGC-1α gene expression

PQ exposure significantly reduced PGC-1α gene expression compared with the Control group (1.337 ± 0.2668 vs. 5.008 ± 0.4231, P<0.0001; Fig. X). PGC-1α expression was significantly higher in the PQ+DSF20 group than in the PQ group (3.785 ± 0.3755, P=0.0017). Among the DSF-treated groups, PGC-1α expression was significantly higher in the PQ+DSF20 group than in the PQ+DSF5 group (P=0.0018). (Fig. 6 b).

3-4: Biochemical assessment of liver injury

Serum liver enzyme levels were significantly elevated following PQ exposure compared with the control group. **ALT** increased from 17.00 ± 1.817 in the control group to 56.80 ± 2.083 in the PQ group (P<0.0001). DSF treatment significantly reduced ALT levels in the PQ+DSF10 and PQ+DSF20 groups compared with PQ alone (P=0.0172 and P=0.0002, respectively). A significant difference was also observed between the PQ+DSF5 and PQ+DSF20 groups (P=0.0254). (Fig. 7 a)

Similarly, **AST** levels were significantly higher in the PQ group than in the control group (290.0 ± 10.84 vs. 100.0 ± 2.739, P<0.0001). AST was significantly reduced in the PQ+DSF20 group compared with PQ (114.0 ± 4.000,

P<0.0001). Significant differences were also observed between PQ+DSF5 and PQ+DSF20 and between PQ+DSF10 and PQ+DSF20 (both P<0.0001). (Fig. 7 b)

ALP levels were also significantly increased by PQ exposure compared with the control group (687.0 ± 34.34 vs. 420.0 ± 17.10, P=0.0003). DSF20 significantly reduced ALP levels compared with PQ (501.0 ± 45.56, P=0.0183). (Fig. 7 c)

3-5: Oxidative stress and antioxidant enzyme activity

PQ exposure significantly impaired antioxidant enzyme activity compared with the control group. **GPx** activity was markedly reduced in the PQ group compared with the control group (6.138 ± 0.6407 vs. 42.25 ± 1.174, P<0.0001). DSF treatment group, **CAT** activity was significantly lower in the PQ group than in the control group (422.1 ± 26.42 vs. 1042 ± 32.46, P<0.0001). CAT activity was significantly increased in the PQ+DSF10 and PQ+DSF20 groups compared with PQ (775.5 ± 30.88 and 931.9 ± 37.56, respectively; both P<0.0001). Significant differences were observed between PQ+DSF5 and PQ+DSF10 (P=0.0002), PQ+DSF5 and PQ+DSF20 (P<0.0001), and PQ+DSF10 and PQ+DSF20 (P=0.0230). (Fig. 7 d-e)

In contrast, **MDA** levels were significantly elevated in the PQ group compared with the control group (34.89 ± 0.9085 vs. 9.118 ± 0.4653, P<0.0001). DSF treatment significantly reduced MDA levels in the PQ+DSF10 and PQ+DSF20 groups compared with PQ (28.85 ± 0.9416, P=0.0029; and 21.33 ± 0.9631, P<0.0001, respectively). Among the DSF-treated groups, MDA levels differed significantly between PQ+DSF5 and PQ+DSF20 (P<0.0001) and between PQ+DSF10 and PQ+DSF20 (P=0.0002), whereas the difference between PQ+DSF5 and PQ+DSF10 was borderline (P=0.0500).ignificantly increased GPx activity in the PQ+DSF10 and PQ+DSF20 groups compared with PQ alone (21.78 ± 2.210 and 25.69 ± 3.616, respectively; both P<0.0001). Significant differences were also observed between PQ+DSF5 and PQ. (Fig. 7 g)

4. Discussion

Paraquat (PQ) remains one of the most widely used herbicides worldwide despite its well-recognized toxicity and restrictions in several countries. In the present study, DSF attenuated PQ-induced hepatic injury and fibrotic remodeling, as demonstrated by improved histopathological findings, reduced lipid peroxidation, restoration of

antioxidant enzyme activities, suppression of NLRP3 gene expression, restoration of PGC-1α expression, and reduced fibrosis scores and fibrotic area. Among the tested doses, 20 mg/kg showed the most consistent protective effects across most outcomes, although 10 mg/kg produced comparable effects on NLRP3 suppression, several histopathological parameters, oxidative stress markers (MDA, GPx, and CAT), and ALT reduction. However, these findings do not establish a definitive optimal therapeutic dose.

4.1 Histopathological findings and hepatic injury

Histopathological examination confirmed that PQ induced severe hepatic injury characterized by lobular destruction, hepatocyte vacuolation, hyalinization, necrotic hepatocytes, central vein and sinusoidal congestion, sinusoidal collapse, and macrophage accumulation, consistent with previous reports describing PQ-induced hepatic injury as a consequence of oxidative stress and inflammatory responses [23, 24]. DSF treatment substantially ameliorated these pathological alterations, particularly at 10 and 20 mg/kg. These doses were associated with reduced lobular destruction, less hepatocyte vacuolation and hyalinization, fewer necrotic hepatocytes, and decreased congestion and macrophage accumulation. Although 5 mg/kg also exerted some protective effects, its efficacy was less consistent across different histological indices.

Similar hepatoprotective effects of DSF have been reported in other experimental models, where it reduced hepatocellular necrosis, inflammatory infiltration, and tissue remodeling [13, 14]. The attenuation of macrophage accumulation in hepatic sinusoids observed at 20 mg/kg is particularly noteworthy, as Kupffer cells and infiltrating macrophages are principal contributors to inflammatory cytokine production and subsequent hepatocellular injury [13, 25]. Together, these findings support the protective effects of DSF against PQ-induced hepatic structural damage. However, the extent to which these histological improvements translate into sustained functional benefits requires further investigation.

In contrast to these protective findings, experimental and clinical evidence indicates that DSF can also induce hepatotoxicity under certain conditions, particularly at higher concentrations, with chronic administration, or in the presence of pre-existing liver disease. A comprehensive review of DSF in liver diseases concluded that while DSF holds promise for broader application, its clinical use is hindered by the risk of inducing pharmacologic liver injury, necessitating careful patient selection and monitoring [12]. This hepatotoxic potential is supported by clinical data: in the DILIN prospective study, DSF was the leading cause of drug-induced liver injury (DILI) among medications

for alcohol use disorder, with 3 of 11 cases being fatal or near-fatal, and severe outcomes were most common in patients with underlying liver disease [10]. A recent case report further illustrated that DSF-induced DILI can manifest as life-threatening acute liver failure even at standard doses (250 mg/day) within the first month of therapy, particularly when initiated in patients with pre-existing alcohol-related liver disease [26]. Mechanistically, the hepatotoxicity of DSF has been linked to its capacity to deplete intracellular glutathione and ATP at higher concentrations, although recent in vivo evidence suggests that at clinically relevant doses, DSF does not exacerbate liver toxicity in healthy rats treated with morphine, but may pose a risk in subjects with pre-existing liver impairment [27]. These observations highlight a narrow therapeutic window for DSF and suggest that the hepatoprotective effects observed in our PQ model may be specific to the dose, duration, and the nature of the toxic insult (i.e., acute oxidative stress). The absence of hepatotoxicity in our study, as reflected by the lack of worsening in histopathological scores even at 20 mg/kg, does not rule out the potential for adverse hepatic reactions in other contexts, with higher doses, or with chronic administration. This duality underscores the need for careful dose selection and hepatic monitoring in any translational application of DSF.

4.2 Oxidative stress

Oxidative stress is a major contributor to PQ-induced hepatic injury. PQ undergoes redox cycling in the mitochondrial respiratory chain, generating superoxide anions and other reactive oxygen species (ROS) that overwhelm cellular antioxidant defenses and initiate lipid peroxidation [23]. In the present study, PQ exposure significantly increased hepatic MDA levels, indicating enhanced lipid peroxidation, and markedly reduced GPx and CAT activities. These findings are consistent with previous evidence showing impaired antioxidant defense and increased lipid peroxidation following PQ exposure, supporting the role of oxidative damage in PQ-induced hepatotoxicity [24]. DSF treatment significantly reduced MDA levels and restored GPx and CAT activities toward the control range, particularly at 10 and 20 mg/kg. The reduction in MDA levels following DSF treatment suggests that decreased lipid peroxidation may contribute to its hepatoprotective effects. However, the interpretation of antioxidant enzyme activities requires caution. In the PQ group, the profound reduction in GPx and CAT activities likely reflects depletion of antioxidant capacity under severe oxidative burden rather than a compensatory response. Following DSF treatment, the restoration of these activities may reflect either recovery of antioxidant capacity or a reduced oxidative burden secondary to other protective mechanisms. Whether DSF directly upregulates GPx and

CAT expression (e.g., via Nrf2-dependent pathways) or indirectly preserves their activity by reducing the oxidative burden remains to be determined. Because antioxidant enzyme activities can reflect both adaptive responses and antioxidant capacity, these findings should not be interpreted as direct evidence of a specific molecular antioxidant mechanism.

Moreover, previous studies have indicated that the effects of DSF on ROS are not uniformly antioxidant and may vary according to cellular context and dose. DSF has been reported to reduce total ROS production primarily through NADPH oxidase-dependent pathways without affecting mitochondrial ROS in some models, whereas in other contexts it may promote ROS accumulation [2, 9]. In the present study, total ROS were not directly measured; therefore, the relative contribution of mitochondrial versus non-mitochondrial ROS to the observed changes in MDA and antioxidant enzyme activities remains to be determined. Therefore, the observed improvement in redox status in our model should be interpreted in conjunction with the histopathological and biochemical findings rather than as evidence of a direct antioxidant action of DSF. The restoration of PGC-1α expression (Section 4.4) may provide a more plausible mechanism by which DSF could enhance mitochondrial antioxidant capacity and reduce ROS production at its source. This possibility is explored in Section 4.4, where the role of PGC-1α in mitochondrial biogenesis and antioxidant defense is discussed.

4.3 NLRP3 inflammasome activation

PQ exposure significantly increased NLRP3 gene expression compared with the control group. DSF treatment significantly reduced NLRP3 expression at 10 and 20 mg/kg, with the lowest expression observed at 20 mg/kg (1.584 ± 0.3673 vs. 5.836 ± 0.5855 in the PQ group; $P<0.0001$). These findings are consistent with the well-established role of ROS as a critical mediator of NLRP3 inflammasome activation [28]. and with the growing body of evidence indicating that DSF inhibits NLRP3 inflammasome activation in hepatic tissue [7, 9, 29].

The mechanistic link between NLRP3 and hepatic fibrosis is now well established. NLRP3 activation promotes hepatocyte pyroptosis and the release of pro-inflammatory cytokines, which in turn drive hepatic stellate cell (HSC) activation and extracellular matrix deposition. Direct evidence for this link comes from studies showing that NLRP3 inflammasome activation within HSCs themselves directly triggers their activation and fibrotic phenotype. In CCl_4-induced liver fibrosis, genetic ablation of NLRP3 abolished the pro-fibrotic effects of PROM2, demonstrating that NLRP3 signaling is a required mediator of fibrotic remodeling in the liver. Pharmacological inhibition of NLRP3

with MCC950 similarly alleviated liver injury and fibrosis in tumor-bearing mice. These observations position NLRP3 not merely as a marker of inflammation, but as a causal driver of the fibrotic cascade, providing a rationale for targeting NLRP3 in PQ-induced hepatic injury [30, 31].

The mechanism by which DSF inhibits NLRP3 has been investigated in several studies. Xu et al. (2024) demonstrated that DSF interferes with NLRP3 palmitoylation at Cys126, thereby preventing its localization to the trans-Golgi network and inflammasome assembly, and showed that DSF inhibits NLRP3 but not NLRC4 in vivo [7]**.** Deng et al. (2020) proposed an alternative or complementary mechanism involving lysosomal membrane protection and reduced cathepsin B release, which limits a key upstream signal for NLRP3 assembly [9]. In our model, the DSF-associated reduction in NLRP3 expression may reflect either direct interference with NLRP3 activation or an indirect consequence of reduced oxidative stress and hepatocellular injury. The observation that NLRP3 suppression was effective at both 10 and 20 mg/kg, whereas fibrosis reduction required 20 mg/kg, suggests that NLRP3 suppression alone may be necessary but not sufficient for reversing fibrotic remodeling, and that additional mechanisms—such as PGC-1α-mediated mitochondrial protection—may be required for measurable antifibrotic effects

4.4 PGC-1α and mitochondrial biogenesis

PGC-1α is a master transcriptional regulator of mitochondrial biogenesis, coordinating the activity of nuclear respiratory factors, activating genes involved in the respiratory chain and fatty acid oxidation, and augmenting mitochondrial respiratory capacity. Beyond its metabolic role, PGC-1α also regulates antioxidant enzyme expression, including Cat, Sod1, Gpx1, and Ucp2, thereby reducing mitochondrial ROS production [32]. In the present study, PQ exposure significantly reduced PGC-1α gene expression ($P<0.0001$), whereas DSF treatment restored PGC-1α expression, with a significant increase observed at 20 mg/kg ($P=0.0017$).

These findings are consistent with previous studies demonstrating that reduced PGC-1α is associated with exacerbated mitochondrial dysfunction, oxidative stress, inflammation, and fibrosis in the liver. Hepatocyte-specific PGC-1α knockout mice develop exacerbated fibrosis following CCl_4 challenge, and PGC-1α silencing aggravates hepatocyte EMT, whereas PGC-1α overexpression mitigates oxidative stress-induced EMT and fibrosis [5]. Moreover, hepatic PGC-1α ablation has been shown to impair oxidative phosphorylation, reduce respiratory capacity, and increase inflammation and fibrosis in MASH models [6]. Conversely, agents that upregulate PGC-

1α—such as neohesperidin via AMPK activation [32] or astaxanthin via FGF21 [33] —improve mitochondrial biogenesis, restore antioxidant defense, and reduce hepatic inflammation and fibrosis.

The DSF-associated restoration of PGC-1α in our model may therefore contribute to the observed reduction in oxidative stress and NLRP3 expression, and to the attenuation of fibrotic remodeling. This interpretation is supported by the observation that PGC-1α can interact with phosphorylated NF-κB p65 and limit IL-6 transcription, thereby reducing M2 macrophage polarization and HSC activation [34]. The restoration of PGC-1α may thus constitute a mechanism by which DSF reduces oxidative stress at its mitochondrial source, complementing the direct inhibition of NLRP3 palmitoylation proposed by Xu et al. (2024) [7] and the lysosomal protection proposed by Deng et al. (2020) [9].

4.5 Fibrotic remodeling

PQ exposure significantly increased hepatic fibrosis, as demonstrated by both the fibrosis score (from 0.06000 ± 0.03393 to 3.717 ± 0.1090; $P<0.0001$) and the percentage of fibrotic area (from 3.221 ± 0.2279% to 17.08 ± 0.7621%; $P<0.0001$). DSF treatment significantly reduced both measures of hepatic fibrosis only at 20 mg/kg (fibrosis score: 0.6269 ± 0.1038; fibrotic area: 10.41 ± 0.5816%; both $P<0.0001$), whereas 5 and 10 mg/kg did not produce statistically significant reductions.

The literature on DSF and fibrosis is notably inconsistent, and this inconsistency directly informs the interpretation of our findings. On the one hand, several studies support antifibrotic efficacy. Yang et al. (2022) demonstrated that low-dose DSF (4 mg/kg) attenuated liver fibrosis in CCl_4 and BDL models by inhibiting HSC activation and proliferation and inducing apoptosis of activated HSCs [14]. In Graves' orbitopathy models, DSF dose-dependently inhibited fibrosis and extracellular matrix production markers (FN1, COL1A1, α-SMA, CTGF) in orbital fibroblasts, partially through the ERK–Snail signaling pathway [35, 36]. In pulmonary fibrosis, DSF exerted antifibrotic effects through reactivation of COX-2–mediated PGE2 biosynthesis (Pei et al., 2023). On the other hand, other studies report conflicting results. Rostami et al. (2025) reported that neither 25 nor 50 mg/kg DSF produced any significant anti-fibrotic effects in a CCl_4 model, despite improvements in hepatocyte morphology and serum enzymes; the authors explicitly concluded that "liver fibrosis didn't change" at these doses [16]. A recent comprehensive review concluded that DSF holds promise for liver disease treatment, but its clinical use is hindered by a narrow therapeutic window and the risk of pharmacologic liver injury at higher doses [12]. Systematic reviews further highlight the

methodological heterogeneity and lack of standardized formulations across preclinical studies, which complicates direct comparisons [1]. These discrepancies highlight the context-dependent nature of DSF's antifibrotic effects and suggest that hepatocellular protection may precede measurable fibrosis regression.

Notably, dose- and tissue-specificity appear to be critical determinants of DSF's antifibrotic efficacy. In a PQ-induced pulmonary fibrosis model, DSF at 10 mg/kg provided the most effective protection, whereas the 100 mg/kg dose had limited benefits, suggesting dose-dependent toxicity [37]. In our own parallel PQ-induced renal injury model, 10 mg/kg was identified as the optimal antifibrotic dose in the kidney [19]. In contrast, the present hepatic study required 20 mg/kg for measurable fibrosis reduction. This discrepancy between renal, pulmonary, and hepatic optimal doses strongly suggests that the therapeutic window of DSF for antifibrotic effects is not only narrow but also tissue-specific, likely reflecting differences in drug distribution, local redox environment, and the relative contribution of distinct fibrogenic cell populations (myofibroblasts in the kidney and lung versus HSCs in the liver). These observations collectively suggest that the reduction in fibrosis observed in our hepatic model at 20 mg/kg is consistent with a tissue-dependent and dose-dependent effect, rather than a uniform antifibrotic action of DSF across organs.

In our study, the reduction in fibrosis at 20 mg/kg was accompanied by the most consistent improvements in histopathology, PGC-1α expression, MDA levels, and AST/ALP, suggesting that the antifibrotic effect of DSF may be secondary to reduced hepatocellular injury, oxidative stress, and inflammation, rather than a direct effect on collagen deposition. This interpretation is further supported by the dissociation between NLRP3 suppression (effective at 10 and 20 mg/kg) and fibrosis reduction (effective only at 20 mg/kg). This dissociation suggests that attenuation of inflammation and inflammasome activation alone may be insufficient to reverse fibrotic remodeling, and that additional mechanisms—such as PGC-1α-mediated improvement of mitochondrial function and reduction of oxidative stress—may be required for measurable antifibrotic effects. The observation that only the 20 mg/kg dose restored PGC-1α expression to a statistically significant extent is consistent with this hypothesis.

The observed reduction in fibrosis could reflect attenuation of fibrotic remodeling during active injury rather than definitive regression of established fibrosis. This distinction is important because the term "fibrotic remodeling" encompasses both the attenuation of ongoing fibrogenic processes and the reversal of established fibrosis, and our data support the former rather than the latter. Although Yang et al. (2022) reported direct antifibrotic effects of DSF

[14], the model, dose, and treatment duration in that study differed from ours, and the possibility that DSF primarily targets hepatocellular viability and inflammatory pathways during established injury—rather than directly affecting collagen deposition—remains consistent with our findings and with those of Rostami et al. (2025) [16].

5. Strengths and Limitations

The present study has several methodological strengths. It integrated histopathological evaluation, serum liver enzyme measurement, oxidative stress assessment, NLRP3 and PGC-1α gene expression analysis, and quantitative fibrosis assessment, providing a broader assessment of DSF-associated hepatic protection than reliance on a single outcome measure. The dose-response design (5, 10, and 20 mg/kg) allowed identification of 20 mg/kg as the most consistent protective dose and revealed that NLRP3 suppression occurred at lower doses (10 mg/kg) than fibrosis reduction (20 mg/kg), a dissociation that provides mechanistic insight into the hierarchy of DSF's effects. Furthermore, comparison with our parallel renal study (Esmaeili et al., 2026) highlights the tissue-specific nature of DSF's antifibrotic window.

Several limitations should be acknowledged. NLRP3 and PGC-1α were assessed at the mRNA level only; definitive markers of inflammasome activation (cleaved caspase-1 p20, mature IL-1β/IL-18, ASC speck) and PGC-1α protein, mitochondrial biogenesis markers, and respiratory capacity were not measured, so causal roles cannot be concluded and the observed changes may be secondary to reduced oxidative stress or hepatocellular injury. GSH, total or mitochondrial ROS, α-SMA, and Nrf2 were not assessed, limiting comprehensive evaluation of redox status and HSC activation. The PQ model represents toxin-induced injury under specific exposure conditions and does not fully reproduce chronic human liver disease, and the durability of protection after treatment cessation was not evaluated. No mechanistic intervention (e.g., NLRP3 or PGC-1α inhibition, hepatocyte-specific knockout) was included in the present study. Future studies should incorporate protein-level assessments—including Western blot analysis of NLRP3, cleaved caspase-1, mature IL-1β/IL-18, PGC-1α, NRF-1, and TFAM—as well as functional mitochondrial assays to establish the causal mechanisms and validate the proposed PGC-1α–mitochondria–NLRP3 axis

6. Conclusion

In conclusion, DSF attenuated PQ-induced hepatic injury and fibrotic remodeling in rats. Its protective effects were associated with reduced lipid peroxidation, restoration of GPx and CAT activities, suppression of NLRP3 gene expression, restoration of PGC-1α expression, and reduced fibrosis scores and fibrotic area, particularly at 20 mg/kg. Among the tested doses, 20 mg/kg showed the most consistent overall protective effects; however, whether this represents the true optimal dose requires confirmation in a wider dose-response study. Because NLRP3 and PGC-1α were assessed only at the gene-expression level, and mitochondrial biogenesis and inflammasome activation markers were not directly measured, the proposed PGC-1α–mitochondria–NLRP3 axis remains a working hypothesis. The dissociation between the dose-response for NLRP3 suppression (effective at 10 and 20 mg/kg) and that for fibrosis reduction (effective only at 20 mg/kg) suggests that attenuation of inflammasome activation alone may be insufficient to reverse fibrotic remodeling, and that PGC-1α-mediated improvement of mitochondrial function and antioxidant capacity may be required for measurable antifibrotic effects. Notably, the optimal antifibrotic dose in the present hepatic study (20 mg/kg) differed from that in our parallel renal study (10 mg/kg), highlighting the tissue-specific nature of DSF's therapeutic window (Esmaeili et al., 2026). Given the narrow therapeutic window of DSF and its potential for rare but severe hepatotoxicity in humans, careful dose selection and hepatic monitoring will be essential for any translational application. Further studies incorporating protein-level assessments (e.g., NLRP3, cleaved caspase-1, mature IL-1β, PGC-1α, NRF-1, TFAM), functional mitochondrial assays, hepatocyte-specific PGC-1α knockout models, and long-term follow-up are required to establish the causal mechanisms and determine whether these effects translate into sustained hepatic protection.

7. Acknowledgments

The authors thank Babol University of Medical Sciences for its support. We are grateful to our colleagues and technical staff for their essential contributions to this work.

8. Funding

This study was financially supported by the Vice-Chancellery for Research and Technology of Babol University of Medical Sciences.

9. Competing Interests

The authors declare that they have no competing interests.

10. Ethics Approval and Consent to Participate

The study protocol was reviewed and approved by the Ethics Committee of Babol University of Medical Sciences (Approval code: IR.MUBABOL.AEC.1403.021). Our study is a preclinical animal study and not a human clinical trial. Therefore, the registration of a clinical trial number does not apply to this work.

11. Competing Interests

The authors declare that they have no competing interests.

12. AI-Assisted:

During the preparation of this manuscript, the AI-assisted language tool DeepSeek was used exclusively to enhance academic writing style and structural clarity. All AI-generated content was subsequently reviewed, edited, and validated by the authors. No AI tools were employed in the study conception, design, data generation, analysis, or interpretation. The authors take full responsibility for the scientific integrity and conclusions of this manuscript.

13. Data Availability Statement:

The datasets generated and/or analyzed during the current study are available from the corresponding author upon reasonable request.

References

1. Lanz J, Biniaz-Harris N, Kuvaldina M, Jain S, Lewis K, Fallon BA (2023) Disulfiram: mechanisms, applications, and challenges. Antibiotics 12(3):524.
2. Guo W, Chen S, Li C, Xu J, Wang L (2022) Application of disulfiram and its metabolites in treatment of inflammatory disorders. Frontiers in Pharmacology 12:795078.
3. Liu Z, Wang X, Li L, Wei G, Zhao M (2020) Hydrogen sulfide protects against paraquat-induced acute liver injury in rats by regulating oxidative stress, mitochondrial function, and inflammation. Oxidative medicine and cellular longevity 2020(1):6325378.

4. Yousefi Z, Rajabi R, Karima S, Nourbakhsh M, Lotfi AS (2025) Protective anti-fibrotic effect of liraglutide and Pirfenidone combination therapy on liver fibrosis in rats: effects on autophagy and NLRP3 inflammasome. BMC gastroenterology 26(1):57.
5. Zhang L, Zhang Y, Chang X, Zhang X (2020) Imbalance in mitochondrial dynamics induced by low PGC-1α expression contributes to hepatocyte EMT and liver fibrosis. Cell death & disease 11(4):226.
6. Arconzo M, Piccinin E, Pasculli E, Cariello M, Loiseau N, Bertrand-Michel J, et al. (2024) Hepatic-specific Pgc-1α ablation drives fibrosis in a MASH model. Liver International 44(10):2738-52.
7. Xu J, Pickard JM, Núñez G (2024) FDA-approved disulfiram inhibits the NLRP3 inflammasome by regulating NLRP3 palmitoylation. Cell reports 43(8).
8. Jiang Q, Jiang M, Lv Y, Zhang X, Wang S, Zhao J (2025) Disulfiram as an anti-inflammatory agent: mechanisms, nano-delivery strategies, and applications in non-oncologic diseases. RSC advances 15(43):36344-64.
9. Deng W, Yang Z, Yue H, Ou Y, Hu W, Sun P (2020) Disulfiram suppresses NLRP3 inflammasome activation to treat peritoneal and gouty inflammation. Free Radical Biology and Medicine 152:8-17.
10. Gopalakrishna H, Ghabril M, Gu J, Li YJ, Fontana RJ, Kleiner DE, et al. (2024) Drug-induced liver injury due to medications for alcohol use disorder: results from the DILIN prospective study. Journal of addiction medicine 19(3):314.
11. Ramer L, Tihy M, Goossens N, Frossard J-L, Rubbia-Brandt L, Spahr L (2020) Disulfiram-Induced Acute Liver Injury. Case reports in hepatology 2020(1):8835647.
12. Xiong W, Tian A, Qian Z, Li J, Mao X (2025) Disulfiram in liver diseases: a double-edged sword. Naunyn-Schmiedeberg's archives of pharmacology 398(5):4875-89.
13. Xu W, Kadoya Y, Sennari K, Islam W, Zhang T, Sawa T, et al. (2023) Disulfiram encapsulated in polymer nanoparticles ameliorates thioacetamide-induced liver injury. Journal of Drug Delivery Science and Technology 88:104981.
14. Yang X-M, Wu Z, Wang X, Zhou Y, Zhu L, Li D, et al. (2022) Disulfiram inhibits liver fibrosis in rats by suppressing hepatic stellate cell activation and viability. BMC Pharmacology and Toxicology 23(1):54.
15. Zhang R, Sun X, Lu H, Zhang X, Zhang M, Ji X, et al. (2025) Akkermansia muciniphila mediated the preventive effect of disulfiram on acute liver injury via PI3K/Akt pathway. Microbial Biotechnology 18(1):e70083.
16. Rostami A, Golchoobian R, Esmaeili Z, Asghari MH, Hafezi N, Babazadeh Z (2025) Can disulfiram modulate liver injury in CCl4-induced fibrosis in rats? Gastroenterology and Hepatology From bed to Bench 18(4):426.
17. Awadalla EA (2012) Efficacy of vitamin C against liver and kidney damage induced by paraquat toxicity. Experimental and toxicologic pathology 64(5):431-4.
18. Ray S, Sengupta A, Ray A (2007) Effects of paraquat on anti-oxidant system in rats. Indian journal of experimental biology 45(5):432.
19. Esmaeili M, Daraei A, Najafzadehvarzi H, Khafri S, Esmaeili Z, Beheshti Y, et al. (2026) Disulfiram attenuates paraquat-induced renal injury and fibrosis accompanied by changes in Smad3 and Smad7 gene expression. Molecular Biology Reports 53(1):1826.

20. Hamad NS, Ghafoor DD, Rasul HO (2026) Sub-acute intraperitoneal quercetin administration causes dose-dependent organ histopathology and oxidative stress in healthy rats: dissociation between serum biomarkers and tissue-level structural injury. Scientific Reports.
21. Zeinvand-Lorestani H, Nili-Ahmadabadi A, Balak F, Hasanzadeh G, Sabzevari O (2018) Protective role of thymoquinone against paraquat-induced hepatotoxicity in mice. Pesticide biochemistry and physiology 148:16-21.
22. Standish R, Cholongitas E, Dhillon A, Burroughs A, Dhillon A (2006) An appraisal of the histopathological assessment of liver fibrosis. Gut 55(4):569-78.
23. Dinis-Oliveira R, Duarte J, Sánchez-Navarro A, Remião F, Bastos M, Carvalho F (2008) Paraquat poisonings: mechanisms of lung toxicity, clinical features, and treatment. Critical reviews in toxicology 38(1):13-71.
24. Gawarammana IB, Buckley NA (2011) Medical management of paraquat ingestion. British journal of clinical pharmacology 72(5):745-57.
25. Miller A, Lombardo GP, Spiccia L, Natale V, Migliorato A, Bednarski M, et al. (2025) Characterization of immune cells in the rat intestinal mucosa and liver involved in inflammation caused by LPS and evaluation of the effects of N-acetylcysteine and disulfiram (well-known sulfur drugs) for this inflammation. Acta Histochemica 127(3):152272.
26. Wangchuk S, Chhetri B, Loo JL (2026) Disulfiram-Induced Hepatotoxicity in a Patient With Alcohol Use Disorder: A Case Report. Clinical Case Reports 14(8):e73209.
27. Zelazewska Z, Lazarczyk M, Paszkiewicz J, Marszalek-Grabska M, Gawel K, Nawrocka A, et al. (2025) The hepatic and developmental toxicity of chronic morphine and disulfiram co-treatment for pain relief-a comprehensive in vitro and in vivo assessment. Toxicology and Applied Pharmacology:117499.
28. Ziehr BK, Macdonald JA (2024) Regulation of NLRPs by reactive oxygen species: A story of crosstalk. Biochimica et Biophysica Acta (BBA)-Molecular Cell Research 1871(8):119823.
29. Xiong W, Li J, Mao X, Qian Z, Tian A, Peng X, et al. (2025) Disulfiram alleviates immune-mediated liver injury by inhibiting pyroptosis in hepatocytes through the NF-κB pathway. European Journal of Pharmacology 992:177352.
30. Inzaugarat ME, Johnson CD, Holtmann TM, McGeough MD, Trautwein C, Papouchado BG, et al. (2019) NLR family pyrin domain-containing 3 inflammasome activation in hepatic stellate cells induces liver fibrosis in mice. Hepatology 69(2):845-59.
31. Guo J, Lin Y, Gong X, Kuang G, Hu J, Du H, et al. (2025) PROM2 exacerbates CCl4-Induced liver fibrosis via NLRP3 inflammasome activation and hepatocyte pyroptosis. Cellular and Molecular Life Sciences 82(1):403.
32. Wang S-w, Sheng H, Bai Y-f, Weng Y-y, Fan X-y, Lou L-j, et al. (2020) Neohesperidin enhances PGC-1α-mediated mitochondrial biogenesis and alleviates hepatic steatosis in high fat diet fed mice. Nutrition & diabetes 10(1):27.
33. Wu L, Mo W, Feng J, Li J, Yu Q, Li S, et al. (2020) Astaxanthin attenuates hepatic damage and mitochondrial dysfunction in non-alcoholic fatty liver disease by up-regulating the FGF21/PGC-1α pathway. British journal of pharmacology 177(16):3760-77.
34. Zhang Y, Zhang L, Zhao Y, He J, Zhang Y, Zhang X (2023) PGC-1α inhibits M2 macrophage polarization and alleviates liver fibrosis following hepatic ischemia reperfusion injury. Cell Death Discovery 9(1):337.

35. Wang X, Yang S, Ye H, Chen J, Shi L, Feng L, et al. (2022) Disulfiram exerts antiadipogenic, anti-inflammatory, and antifibrotic therapeutic effects in an in vitro model of Graves' orbitopathy. Thyroid® 32(3):294-305.
36. Wang X, Ye H, Yang S, Sha X, Wang X, Zhang T, et al. (2022) Disulfiram exerts antifibrotic and anti-inflammatory therapeutic effects on perimysial orbital fibroblasts in Graves' orbitopathy. International Journal of Molecular Sciences 23(9):5261.
37. Karimzadeh F, Daraei A, Zabihi-Neyshaburi E, Feizi F, Ranaee M, Khafri S, et al. (2025) Repurposing disulfiram: targeting Zeb1 to attenuate paraquat-induced pulmonary fibrosis in rats. Journal of Molecular Histology 56(5):318.

Figure legend

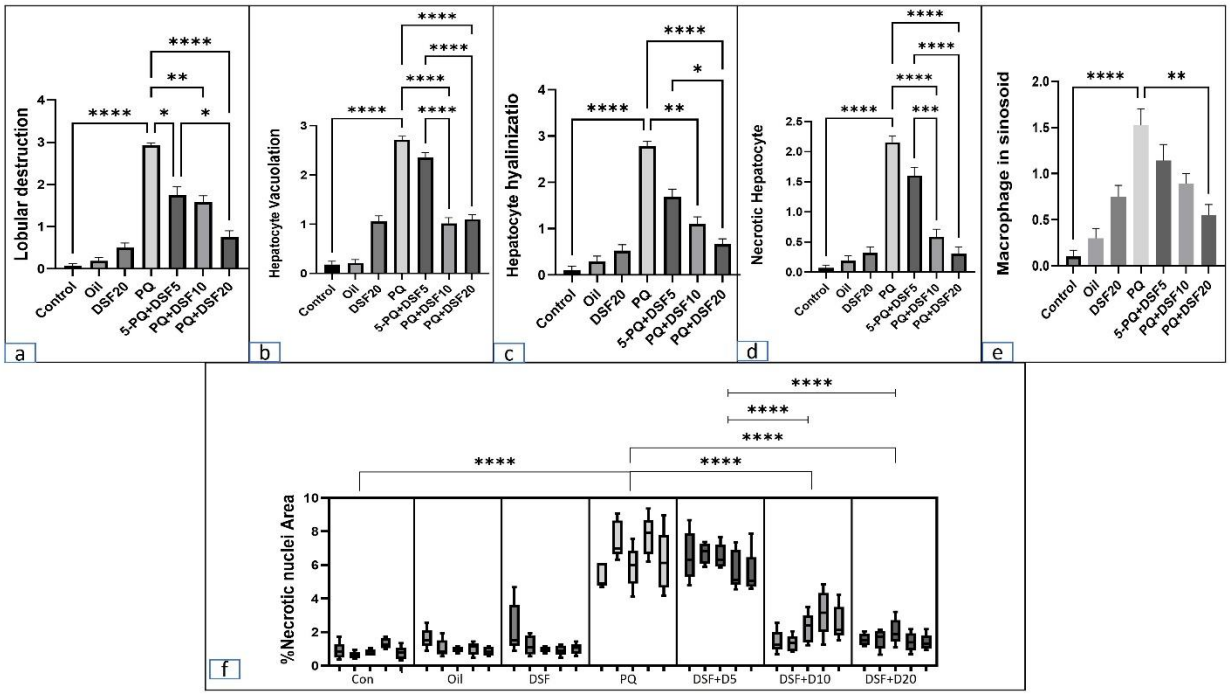


Figure 1: Histopathological assessment of the protective effects of DSF against PQ-induced hepatic injury in a rodent model.

(a–e) Bar graphs showing the histopathological scoring of liver injury across experimental groups: Control, Oil, DSF20, PQ, and combination treatment groups (5-PQ+DSF5, PQ+DSF10, and PQ+DSF20). Evaluated parameters include lobular destruction (a), hepatocyte vacuolation (b), hepatocyte hyalinization (c), necrotic hepatocytes (d), and macrophage infiltration in sinusoids (e). **(f)** Box-and-whisker plot quantifying the percentage of necrotic nuclei area across Control, Oil, DSF, PQ, and combination treatment groups (DSF+D5, DSF+D10, and DSF+D20). Data are presented as mean ± SEM for bar graphs and median with interquartile range for the box plot. Statistical significance is indicated by asterisks (*$p < 0.05$, **$p < 0.01$, ****$p < 0.0001$).

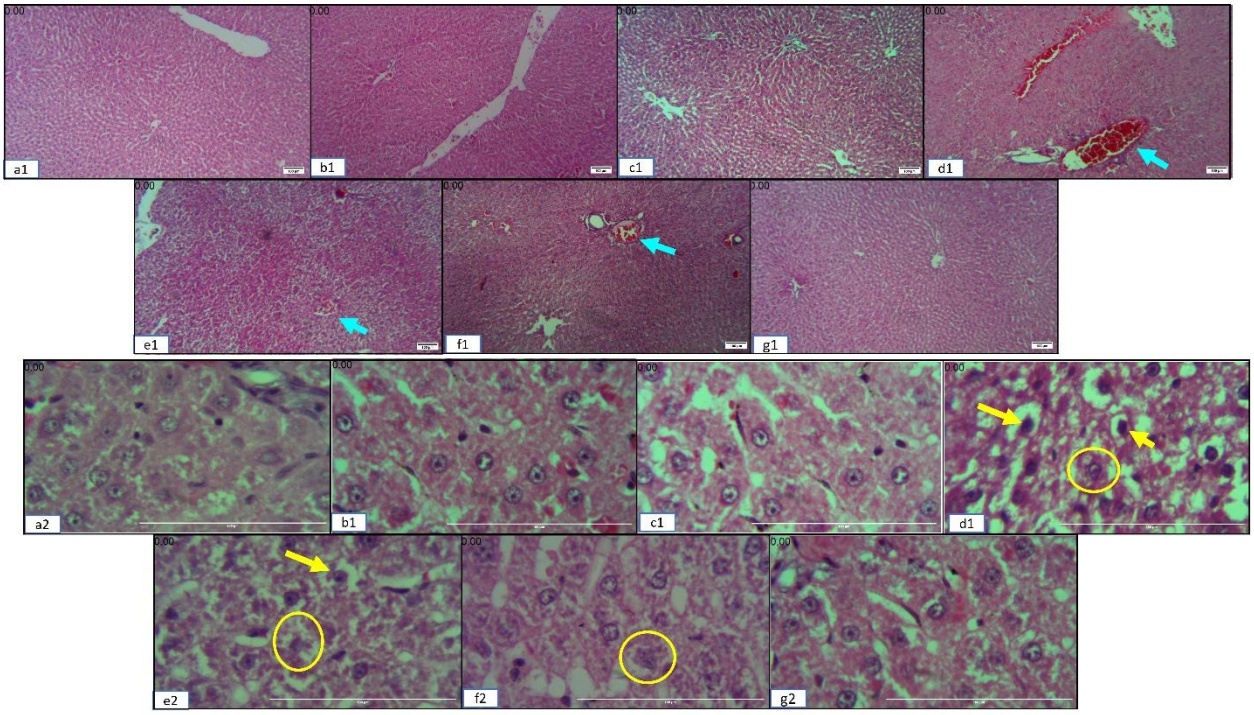


Figure 2. Representative histopathological features of liver tissue following paraquat exposure and disulfiram treatment.

Representative hematoxylin and eosin (H&E)-stained liver sections from the Control (a), Vehicle (b), DSF20 (c), PQ (d), PQ+DSF5 (e), PQ+DSF10 (f), and PQ+DSF20 (g) groups. Panels a1–g1 show the overall hepatic architecture at 18× magnification. Blue arrows indicate areas of vascular congestion. Panels a2–g2 show hepatocytes at 180× magnification. Yellow circles indicate hepatocellular vacuolation, and yellow arrows indicate hepatocytes with pyknotic/necrotic nuclei. Scale bars = 100 μm.

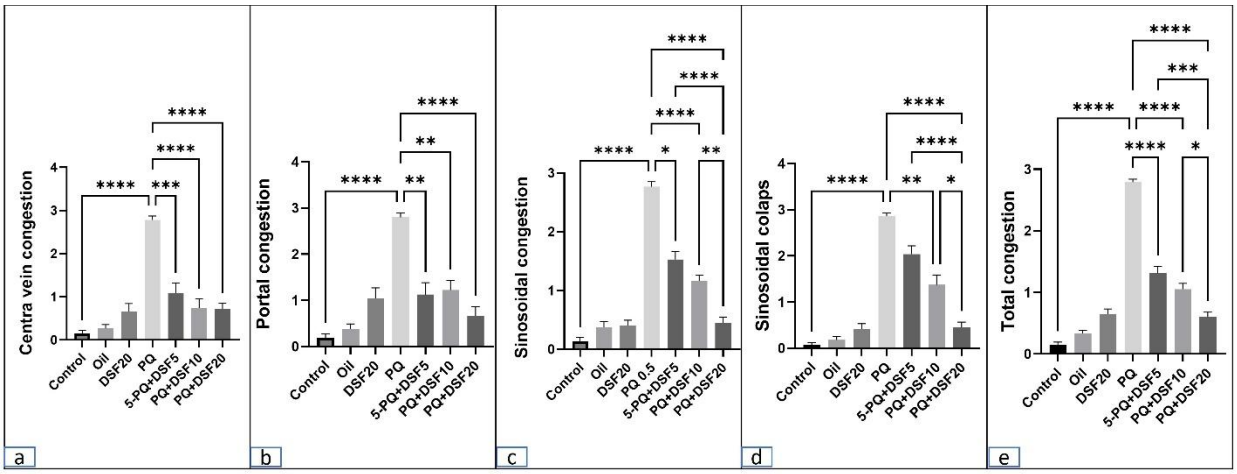


Figure 3. Histopathological evaluation of the ameliorative effects of DSF on Paraquat-induced hepatic vascular congestion.

(a–e) Bar graphs showing the histopathological scoring across experimental groups: Control, Oil, DSF20, PQ, and combination treatment groups (5-PQ+DSF5, PQ+DSF10, and PQ+DSF20). Evaluated parameters include Central vein congestion (a), Portal congestion (b), Sinusoidal congestion (c), Sinusoidal collapse (d), and Total congestion (e). Data are presented as mean ± SEM. Statistical significance between groups is indicated by asterisks (*$p < 0.05$, **$p < 0.01$, ***$p < 0.001$, and ****$p < 0.0001$).

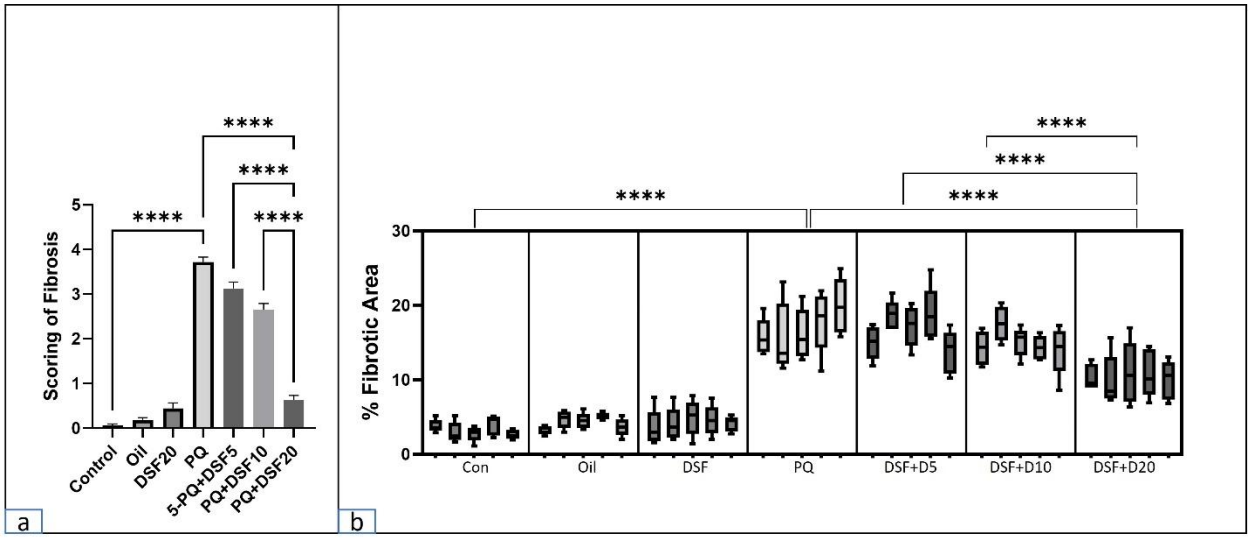


Figure 4. Ameliorative effects of DSF on PQ-induced hepatic fibrosis in a rodent model.

(a) Bar graph showing the Scoring of Fibrosis across experimental groups: Control, Oil, DSF20, PQ, and combination treatment groups (5-PQ+DSF5, PQ+DSF10, and PQ+DSF20).

(b) Box-and-whisker plot displaying the % Fibrotic Area across Control (Con), Oil, DSF, PQ, and combination treatment groups (DSF+D5, DSF+D10, and DSF+D20).

Data are presented as mean ± SEM for panel (a) and median with interquartile range for panel (b). Statistical significance is indicated by asterisks (****$p < 0.0001$).

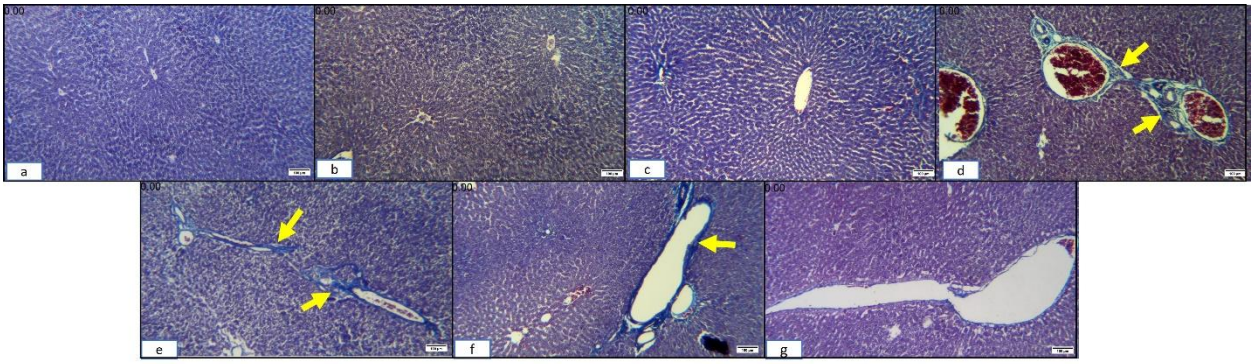


Figure 5. Representative Masson's trichrome-stained liver sections showing hepatic fibrosis. Representative liver sections from the Control (a), Vehicle (b), DSF20 (c), PQ (d), PQ+DSF5 (e), PQ+DSF10 (f), and PQ+DSF20 (g) groups. Blue-stained areas indicate collagen deposition, and yellow arrows indicate areas of hepatic fibrosis. All images were obtained at 4× magnification. Scale bars = 100 μm.

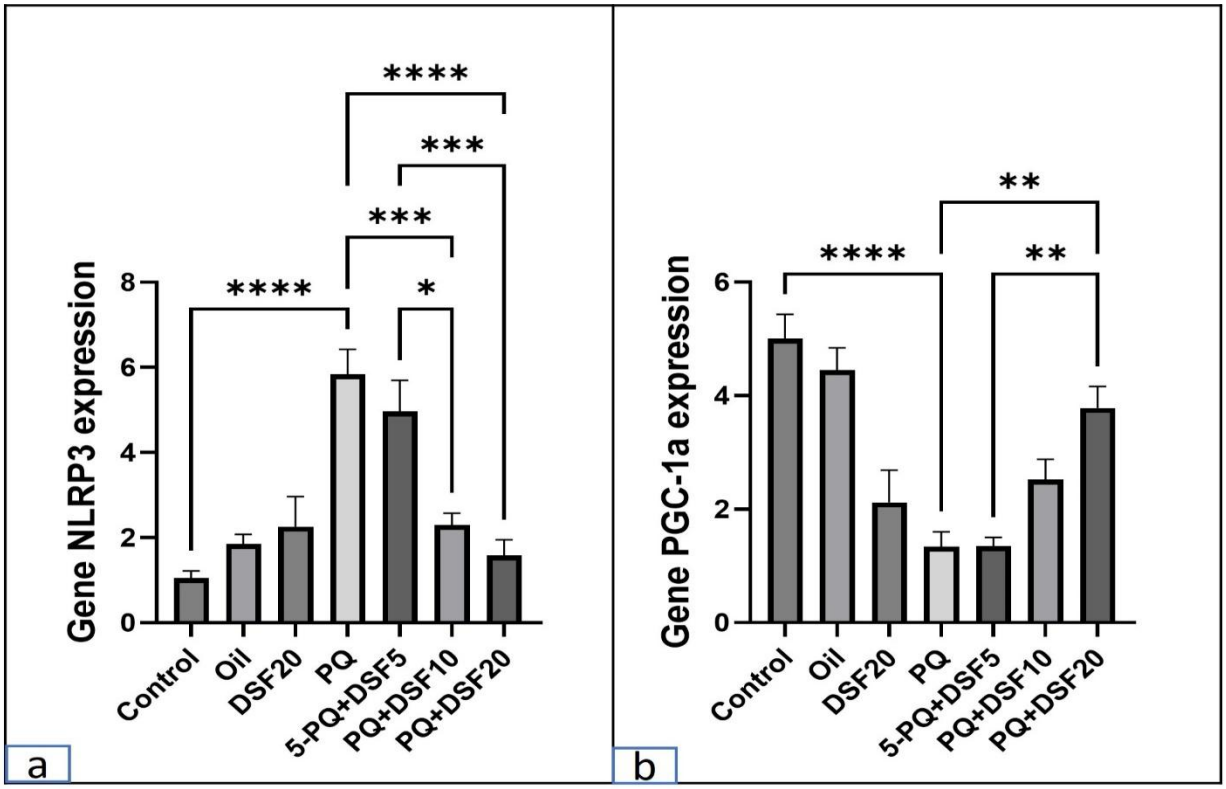


Figure 6: Modulatory effects of DSF on hepatic NLRP3 and PGC-1α gene expression in PQ-induced toxicity**.**

(a) Bar graph showing the relative mRNA expression of the NLRP3 gene (inflammatory marker) across experimental groups. Paraquat (PQ) exposure significantly upregulated NLRP3 expression compared to the Control group, whereas Dexamethasone treatment (particularly at PQ+DSF20) significantly downregulated its expression. (b) Bar graph displaying the relative mRNA expression of the PGC-1α gene (mitochondrial biogenesis and antioxidant marker). PQ significantly downregulated PGC-1α expression, while Dexamethasone treatment (especially at PQ+DSF20) significantly restored its expression to levels comparable to the Control group. Data are presented as mean ± SEM. Statistical significance between groups is indicated by asterisks (*$p < 0.05$, **$p < 0.01$, ***$p < 0.001$, and ****$p < 0.0001$).

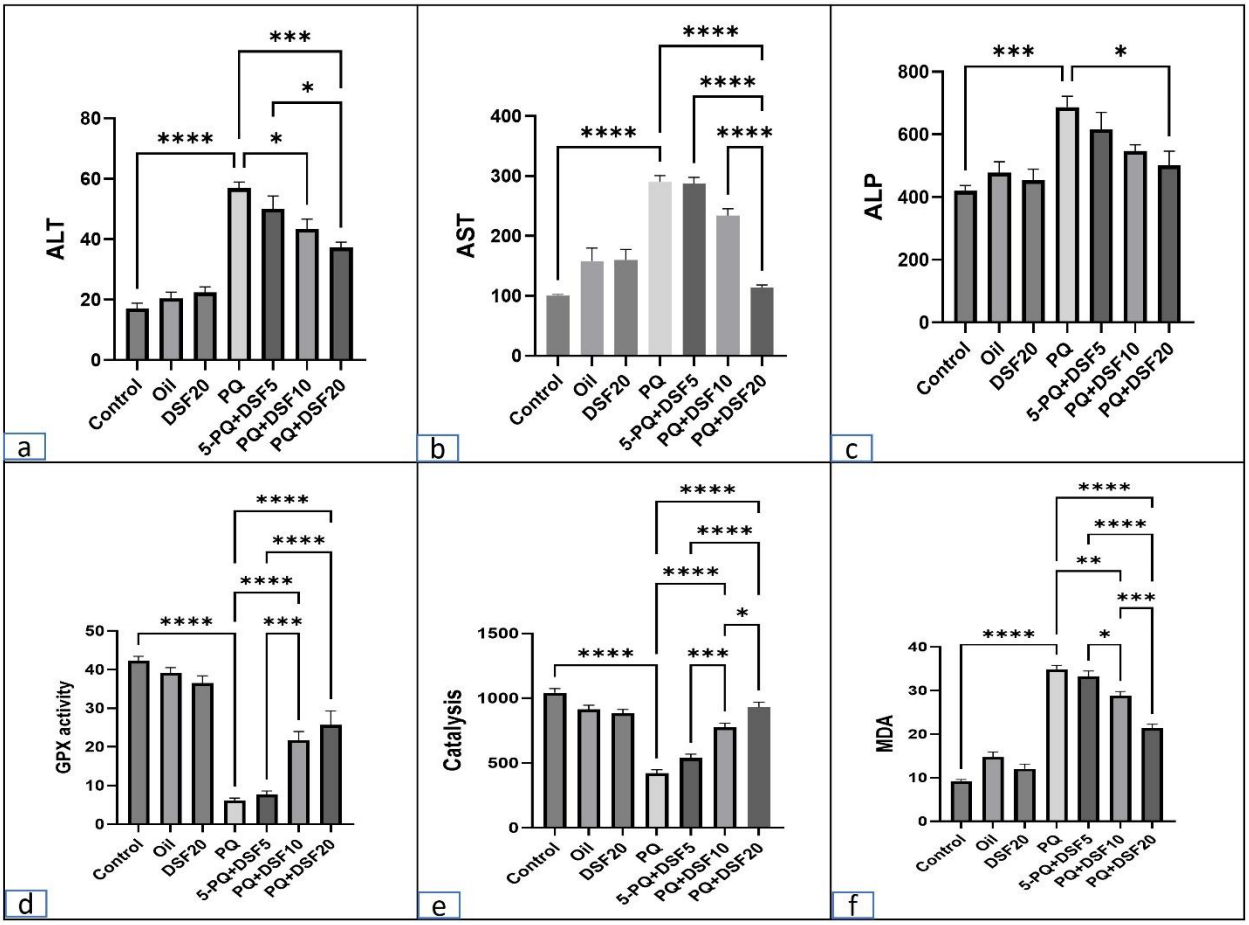


Figure 7: Ameliorative effects of DSF on PQ-induced hepatic dysfunction and oxidative stress in a rodent model.

(a–c) Serum levels of liver function enzymes, including ALT, AST, and ALP, across experimental groups. PQ exposure significantly elevated these enzymes compared to the Control group, whereas DSF treatment significantly attenuated their levels.

(d–e) Hepatic antioxidant enzyme activities, including GPx and Catalase. PQ significantly depleted the activities of these enzymes, while DSF treatment significantly restored their activities.

(f) MDA levels, as an indicator of lipid peroxidation. PQ exposure significantly increased MDA levels, whereas Dexamethasone treatment significantly reduced them.

Data are presented as mean ± SEM. Statistical significance between groups is indicated by asterisks (*$p < 0.05$, **$p < 0.01$, ***$p < 0.001$, and ****$p < 0.0001$).

Supplementary Files

This is a list of supplementary files associated with this preprint. Click to download.

- LiverHistopathology.pptx